Mar Geophys Res (2017) 38:71–83
DOI 10.1007/s11001-016-9279-y

ORIGINAL RESEARCH PAPER

$^{230}Th/^{238}U$ dating of hydrothermal sulfides from Duanqiao hydrothermal field, Southwest Indian Ridge

Weifang Yang[1,2] · Chunhui Tao[2,3] · Huaiming Li[2] · Jin Liang[2] · Shili Liao[2] · Jiangping Long[1,2] · Zhibang Ma[4] · Lisheng Wang[4]

Received: 16 May 2016 / Accepted: 4 August 2016 / Published online: 5 November 2016

Abstract Duanqiao hydrothermal field is located between the Indomed and Gallieni fracture zones at the central volcano, at 50°28′E in the ultraslow-spreading Southwest Indian Ridge (SWIR). Twenty-eight subsamples from a relict chimney and massive sulfides were dated using the $^{230}Th/^{238}U$ method. Four main episodes of hydrothermal activity were determined according to the restricted results: 68.9–84.3, 43.9–48.4, 25.3–34.8, and 0.7–17.3 kyrs. Hydrothermal activity of Duanqiao probably started about 84.3 (±0.5) kyrs ago and ceased about 0.737 (±0.023) kyrs ago. The periodic character of hydrothermal activity may be related to the heat source provided by the interaction of local magmatism and tectonism. The estimated mean growth rate of the sulfide chimney is <0.02 mm/yr. This study is the first to estimate the growth rate of chimneys in the SWIR. The maximum age of the relict chimney in Duanqiao hydrothermal filed is close to that of the chimneys from Mt. Jourdanne (70 kyrs). The hydrothermal activity in Dragon Flag field is much more recent than that of Duanqiao or Mt. Jourdanne fields. The massive sulfides are younger than the sulfides from other hydrothermal fields such as Rainbow, Sonne and Ashadze-2. The preliminarily estimated reserves of sulfide ores of Duanqiao are approximately 0.5–2.9 million tons.

Keywords Southwest Indian Ridge (SWIR) · Duanqiao · Hydrothermal sulfides · $^{230}Th/^{238}U$ dating · Hydrothermal activity · Growth rate

Introduction

The $^{230}Th/^{238}U$ dating method was widely applied to determine the age of seafloor hydrothermal sulfides (Lalou et al. 1985, 1993, 1995, 1998a, b). This method is usually used for dating samples aged between 5 and 350 kyrs (Lalou et al. 1993; Lalou and Brichet 1987). The development of analytic techniques has greatly improved the dating precision in the age range from 10 to 600 kyrs by multi-collector inductively coupled plasma mass (MC-ICP-MS) (Cheng et al. 2013; Shen et al. 2008, 2013; Ludwig et al. 2011; Andersen et al. 2008). When applying the $^{230}Th/^{238}U$ dating method, two assumptions are made: the negligible initial ^{230}Th and closed system decay after mineral formation (Lalou et al. 1985, 1986). Other U–Th disequilibrium methods such as $^{226}Ra/^{210}Pb$, $^{228}Ra/^{228}Th$ and $^{210}Pb/Pb$ were used to determine the age of deposits <150 years (Lalou et al. 1986; Jamieson et al. 2013). While the ESR (electron spin resonance) dating of barite ($^{226}Ra/^{228}Ra$) in seafloor hydrothermal fields can obtain ages of 300–3620 years (Kasuya et al. 1991; Okumura et al. 2010). So far, the $^{230}Th/^{238}U$ dating was used to obtain the ages of seafloor massive sulfide deposits from the East Pacific Ridge (EPR), the Mid-Atlantic Ridge (MAR) and the Central Indian Ridge (CIR) (Lalou and Brichet 1982, 1986, 1988, 1998a, b; You and Bickle 1998; Kuznetsov et al. 2006, 2007, 2011, 2013, 2015; Münch et al. 1999; Wang et al. 2012). The limited data established Trans-Atlantic Geotraverse (TAG) as

✉ Chunhui Tao
taochunhuimail@163.com

1 School of Earth Sciences, Zhejiang University, Hangzhou 310010, China

2 Key Laboratory of Submarine Geosciences, Second Institute of Oceanography, State Oceanic Administration, Hangzhou 310012, China

3 Ocean College, Zhejiang University, Hangzhou 310058, China

4 Institute of Geology and Geophysics, Chinese Academy of Sciences, Beijing 100029, China

one of the longest-lived active vent field with a maximum age of 50 kyrs (Lalou et al. 1995; You and Bickle 1998). The data suggests that the lifespan of a hydrothermal deposit is on a scale of 10^5 years.

In the Southwest Indian Ridge, $^{230}Th/^{238}U$ dating has only been used on sulfides from Mt. Jourdanne hydrothermal field. The evolution history of Mt. Jourdanne has been reconstructed and the hydrothermal activities has been indicated (Münch et al. 2001). Duanqiao hydrothermal filed is located between the Indomed Fracture Zone (FZ) and Gallieni FZ at the central volcano at 50°28′E on the SWIR. It was first discovered by the *R/V Dayangyihao* cruise in 2008 (Tao et al. 2012). Previous studies of Duanqiao hydorhermal field were mainly focused on geophysics and molecule biology. Sauter et al. (2004) investigated the relationships between the segmentation and the magnetic structure of the SWIR. A unique segment centered at 50°28′E shows obviously low magnetic anomaly at its center. Li et al. (2015) used three-dimensional seismic tomography at 50°28′E and revealed a low-velocity anomaly (~0.6 km/s) which was accompanied by an unusually thick crust (~9.5 km). Niu et al. (2015) also identified the thick crust (~10 km) beneath the segment center by wide-angle seismic reflection. Li et al. (2013) reported the geochemical and molecular biological compositions of low-temperature hydrothermal deposits. Sun et al. (2015) further investigated the mineralization of these deposits indicating the presence of Fe-oxidizing bacteria. However there is no study aimed at the age of sulfides from this hydrothermal field. And there is no information about when the hydrothermal activity happened.

During the *R/V Dayangyihao* cruises DY115-20 in 2008 and DY125-34 in 2015, several hydrothermal sulfides (including a relict sulfide chimney and massive sulfides) were recovered by TV-guided grab at Duanqiao hydrothermal field. In this study, a complementary $^{230}Th/^{238}U$ geochronological study of hydrothermal sulfides from the hydrothermal field was done. The hydrothermal activity of the field was discussed. The age distribution of the relict chimney and its growth history were also discussed.

Geological setting

The SWIR extends from the Bouvet Triple Junction (54°50′S, 00°40′W) in the South Atlantic Ocean to the Rodrigues Triple Junction (25°30′S,70°00′E) in the Indian Ocean with a distance of about 8000 km, representing more than 10 % of the total length of the global mid-ocean ridge. It separates the African and Antarctic plates. It is an ultraslow-spreading ridge (Dick et al. 2003) with a full spreading rate of ~13–16 mm/yr (Georgen et al. 2003). The average thickness of the crust is 4 km which is much thinner than the average thickness of the ocean crust (about 7 km) (Baker and German 2004). However, beneath the central volcano the crust is as thick as ~9.5 km (Li et al. 2015). The ultraslow-spreading SWIR is characterized by ridge segmentation and non-magmatism (Cannat et al. 2003; Sauter and Cannat 2010). The ridge segment between the Gallieni fracture zone FZ (52°20′E) and Indomed FZ (46°E) is situated in the central shallow portion of the SWIR (Fig. 1a). Geophysical survey results

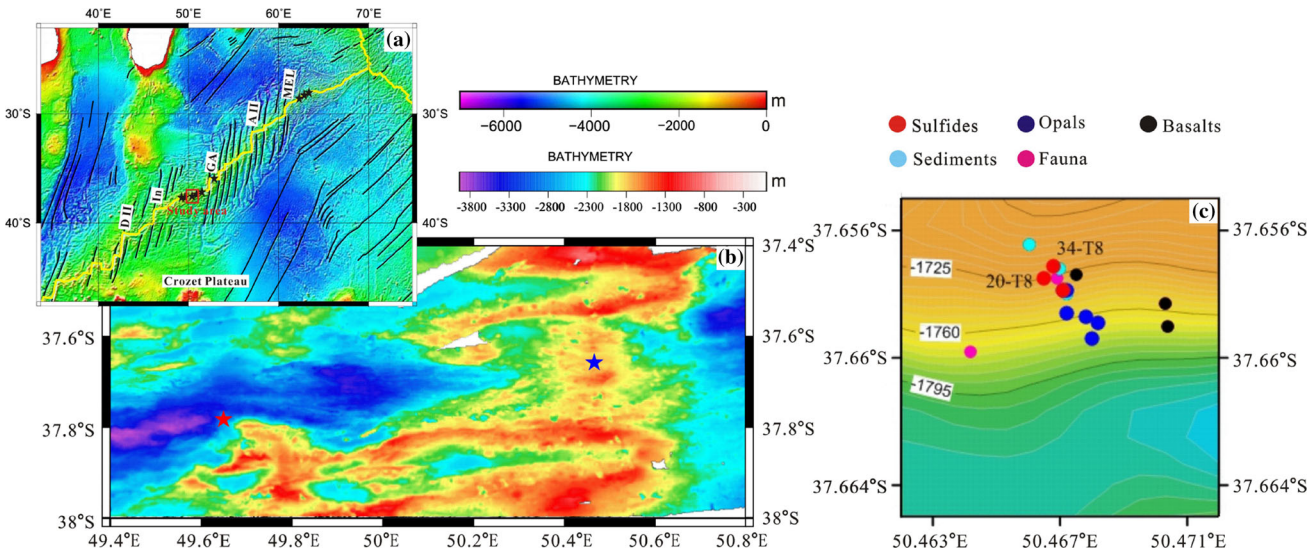

Fig. 1 Topographic map of the Southwest Indian Ridge (SWIR), from Meyzen et al. (2005), showing the locations of sampling sites. **a** Bathymetric map of SWIR. The *red square* indicates the study area. *Black starts* show the hydrothermal fields. DII, Discovery II FZ; In, Indomed FZ; GA, Gallieni FZ; AII, Atlantis II FZ; MEL, Melville FZ; FZ, fracture zone. **b** Bathymetric map of the study area. The *red* and *blue stars* represent the active and inactive filed respectively. **c** Sampling locations. The *red*, *blue*, *black*, *cyan* and *yellow circles* represent the sulfides, opals, basalts, sediments and fauna stations, respectively

show that this region has experienced a dramatic increase in magma supply since 8–10 Ma (Sauter et al. 2004, 2009). The combined effects of magma supply, thermal sources of magmatic activities, unique tectonic setting and hotspots, make hydrothermal system and sulfide mineralization along the SWIR are extremely complicated (Georgen et al. 2001; Sauter et al. 2009; Tao et al. 2014).

Duanqiao hydrothermal field (50°28′E) was detected by deep-tow video imaging and measurements of weak Eh, pH, and H_2S anomalies, and it is ~200 m × 125 m in extent, similar to the S zone at Dragon Flag hydrothermal field (Tao et al. 2012) (Fig. 1b). Hydrothermal sulfides including relict chimneys and massive sulfides, opals, basalts, metalliferous sediments, and relicts of hydrothermal vent fauna including abundant molluscs and gastropod shells are pervasive in the field (Fig. 1c).

Sample description

Two TV guided grab stations were carried out on Duanqiao hydrothermal field during the DY115-20 and DY125-34 cruises of R/V Dayang Yihao in 2008 and 2015. The relict inactive chimney and the massive sulfides were collected by TV grab during the DY125-34 cruise and DY115-20 cruises, respectively. All the sulfides lie at the depth between 1720 and 1780 m (Fig. 1c). Two cross-sections of the relict chimney (34-T8-1 and 34-T8-2) and two massive sulfides (20-T8-1 and 20-T8-4) were selected for $^{230}Th/^{238}U$ dating.

Both of the two chimney cross-sections have central conduits filled with sphalerite and pyrite. The diameter of conduits ranges from 0.3 to 1 cm. The chimney cross-sections were cut into pieces for analysis (Fig. 2a, b). The massive sulfides were also sub-sampled by micro-drilling (Fig. 2c, d). The mineral assemblages of all the samples consist mainly of chalcopyrite, sphalerite, pyrite and marcasite. Sphalerite and pyrite are commonly replaced by chalcopyrite.

Analytical methods

Twenty-eight sub-samples were selected for $^{230}Th/^{238}U$ dating. U and Th chemical separations and the mass spectrometry analysis were performed at the U-series chronology lab of Institute of Geology and Geophysics (IGG), Chinese Academy of Sciences. The chemical separation procedures were similar to those described in Edwards et al. (1987) and Cheng et al. (2013). About 30–300 mg of the powered samples were weighted in an acid-cleaned Teflon beaker, and dissolved first in HNO_3, then in HF and $HClO_4$ to ensure that the samples were completely dissolved. As yield tracer, ^{229}Th–^{233}U–^{236}U spike were added to the sample solutions. After adding two drops of $HClO_4$, the samples were caped and heated for 12 h at 100 °C to remove organic matter and equilibrate the spike with sample. Uranium and Thorium were separated using Fe-coprecipitation and ion-exchang chromatography (2.5 ml columns with BioRad AG1-X8, 100–200 mesh). After removing the other metal ions with 7 M HNO_3, thorium was eluted off the column with 8 M HCl, and uranium was eluted by 0.1 M HNO_3. The purified U and Th fractions were evaporated until dry and taken up with 2 % HNO_3 + 0.1 % HF, and then stored in acid-cleaned plastic ICP-vials. Procedural blanks were measured regularly and nine-month average values were 8.6 pg ^{238}U, 0.05 pg ^{238}U and 0.2 pg ^{232}Th (Wang et al. 2016). A gravimetric U solution was also prepared by dissolving a weighted piece of NBS-CRM-112A metal, obtained from New Brunswick Laboratories. The $^{234}U/^{238}U$ ratio is $(52.841 \pm 0.082) \times 10^{-6}$, and $\delta^{234}U$ is (−38.7 ± 1.5) ‰ (Cheng et al. 2000, 2013; Wang et al. 2016). HU-1(Harwell Uraninite) and NBS Th were used as the standard for U and Th (Wang et al. 2016).

All the samples were analyzed using a Thermo Fisher NEPTUNE MC-ICP-MS at IGG. The collected U and Th were introduced to CETAC Aridus II atomization room by PFA ESI-50 atomizer. The U and Th were then heated and atomized to aerosol and introduced to the mass spectrometer with argon and nitrogen. The argon flow rates were set at 16 l/min for plasma gas, 0.78 l/min for auxiliary gas and 0.8–1.1 l/min for the sample gas. The Neptune was operated at low resolution (M/ΔM = 300). The abundance sensitivity behind the retarding potential quadrupole (RPQ) is about 3–5 × 10^{-7} (Cheng et al. 2013; Wang et al. 2016). All the U and Th isotopes were measured by secondary electron multiplier (SEM). The detailed parameters of the mass spectrometer can be found in Wang et al. (2016) or Cheng et al. (2013). The age of the samples can be calculated using the following Eqs. (1) and (2) by measuring the present-day activity ratios of $^{230}Th/^{238}U$ and $^{234}U/^{238}U$ (Edwards et al. 1987):

$$\left(\frac{^{230}Th}{^{238}U}\right)_{activity} - 1 = -e^{-\lambda_{230}t} + \frac{\delta^{234}U_{measured}}{1000} \times \frac{\lambda_{230}}{\lambda_{230} - \lambda_{234}}\left[1 - e^{-(\lambda_{230}-\lambda_{234})t}\right] \quad (1)$$

where $\boldsymbol{\lambda_{230}}$ and $\boldsymbol{\lambda_{234}}$ represent the decay constants of ^{230}Th and ^{234}U, respectively, and $\boldsymbol{t}$ is the age of sample.

The $\frac{^{234}U}{^{238}U}$ ratio is expressed in δ–n, where

$$\delta^{234}U_{measured} = \left\{\left[\left(\frac{^{234}U}{^{238}U}\right)_{activity} / \left(\frac{^{234}U}{^{238}U}\right)_{equilibrium}\right] - 1\right\} \times 1000 \quad (2)$$

$\delta^{234}U_{initial}$ was calculated based on the ^{230}Th age (t):

$$\delta^{234}U_{initial} = \delta^{234}U_{measured} \times e^{\lambda_{234}t} \quad (3)$$

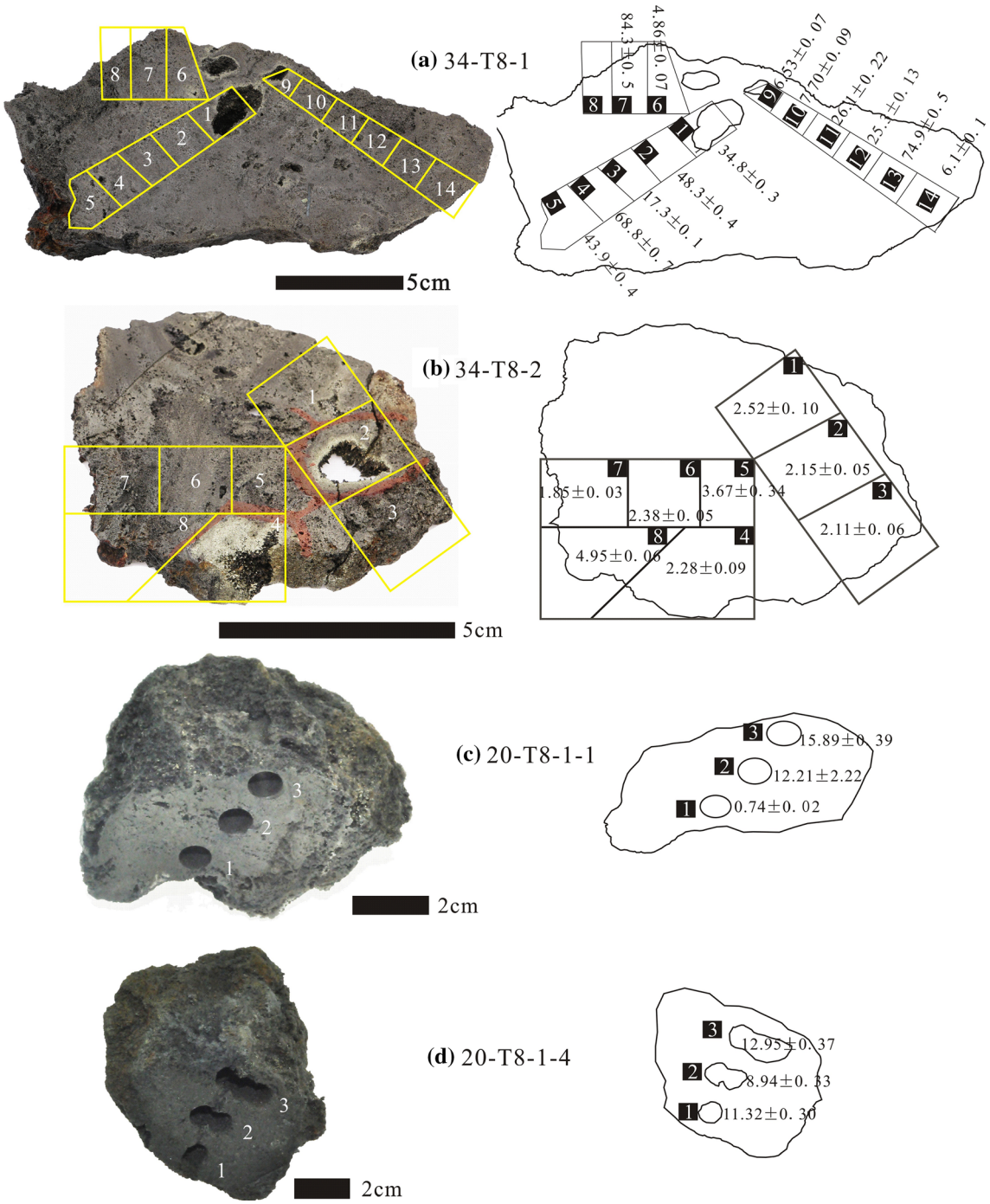

Fig. 2 **a** Chimney section of 34-T8-1 and age distribution of each part. The distance separating the center of sub-samples 9 and 14 is about 8 cm. **b** Chimney section of 34-T8-2 and age distribution of each part. **c**, **d** Overview of massive sulfide samples from Duanqiao hydrothermal field. The *number* represents each part of the chimney sections or massive sulfides analyzed for this study. *Time scale* kyrs

Results

The U–Th isotope systematic of the samples and their ^{230}Th ages are given in Table 1. The ^{238}U concentrations of sulfides range from 22.53 (±0.03) to 948.72 (±1.53) ppb and the ^{232}Th concentrations vary from 140 (±3) to 3363 (±68) ppt (Table 1). In general, the ^{232}Th concentrations are very low with samples 34-T8-2-1 and 20-T8-1-3 having the lowest concentrations.

As shown in Fig. 3 and Table 1, there is no systematic relation between the U content and the age of the samples. The samples with low U contents yield some of the older ages as well as younger ages. The U contents of sample 34-T8-1-1 (64.60 ± 0.12 ppb), 34-T8-1-2

Table 1 U and Th data and ^{230}Th ages for relict chimneys and massive sulfides samples from Duanqiao hydrothermal field

Sample number	^{238}U (ppb)	^{232}Th (ppt)	δ^{234}U measured[a]	[^{230}Th/^{238}U] activity[b]	[^{230}Th/^{232}Th] 10^{-6}[c]	^{230}Th Age (yr) uncorrected	^{230}Th Age (yr) corrected[d]	$\delta^{234}U_{Initial}$ corrected[e]
34-T8-1-1	64.60 ± 0.12	334 ± 7	104.2 ± 2.4	0.3043 ± 0.0021	955.7 ± 20.4	34,970 ± 302	34,833 ± 317	115 ± 3
34-T8-1-2	133.61 ± 0.23	332 ± 7	239.6 ± 2.2	0.4503 ± 0.0028	2966.9 ± 62.5	48,441 ± 392	48,384 ± 394	275 ± 3
34-T8-1-3	139.27 ± 0.23	305 ± 6	220.3 ± 2.3	0.1803 ± 0.0013	1358.6 ± 29.0	17,351 ± 138	17,300 ± 143	231 ± 2
34-T8-1-4	301.21 ± 0.53	1120 ± 23	187.3 ± 2.3	0.5644 ± 0.0043	2502 ± 53.5	68,927 ± 738	68,839 ± 740	227 ± 3
34-T8-1-5	379.21 ± 0.72	3363 ± 68	133.7 ± 2.3	0.3803 ± 0.0028	707.1 ± 15.1	44,173 ± 417	43,948 ± 445	151 ± 3
34-T8-1-6	124.95 ± 0.20	343 ± 7	131.6 ± 1.9	0.05 ± 0.0005	297.9 ± 6.7	4929 ± 53	4857 ± 73	133 ± 2
34-T8-1-7	211.85 ± 0.35	769 ± 15	271.5 ± 2.1	0.7016 ± 0.0028	3186.5 ± 65.0	84,416 ± 531	84,338 ± 534	344 ± 3
34-T8-1-9	948.72 ± 1.53	2998 ± 60	132 ± 2.0	0.0666 ± 0.0005	347.2 ± 7.4	6607 ± 49	6526 ± 75	134 ± 2
34-T8-1-10	82.31 ± 0.35	244 ± 5	134.3 ± 2.1	0.0782 ± 0.0007	435.6 ± 9.5	7777 ± 70	7701 ± 88	137 ± 2
34-T8-1-11	79.88 ± 0.12	257 ± 5	177.3 ± 1.9	0.2527 ± 0.0018	1294 ± 27.7	26,183 ± 213	26,104 ± 220	191 ± 2
34-T8-1-12	158.38 ± 0.36	306 ± 6	158.4 ± 2.3	0.2418 ± 0.0009	2062.6 ± 42.3	25,389 ± 126	25,341 ± 130	170 ± 2
34-T8-1-13	108.57 ± 0.21	1445 ± 29	471.7 ± 2.6	0.756 ± 0.00339	937.5 ± 19.2	75,209 ± 490	74,964 ± 519	583 ± 3
34-T8-1-14	74.35 ± 0.21	253 ± 5	138.3 ± 2.1	0.0632 ± 0.0008	306 ± 7.2	6227 ± 80	6140 ± 101	141 ± 2
34-T8-2-1	73.65 ± 0.24	168 ± 3	148.8 ± 4.1	0.0268 ± 0.0010	194.5 ± 8.0	2575 ± 94	2518 ± 102	150 ± 4
34-T8-2-2	163.52 ± 0.46	260 ± 5	146 ± 3.1	0.0228 ± 0.0004	234.9 ± 6.1	2191 ± 36	2150 ± 46	147 ± 3
34-T8-2-3	172.23 ± 0.36	337 ± 7	119.5 ± 1.8	0.022 ± 0.0004	185 ± 5.2	2163 ± 43	2112 ± 56	120 ± 2
34-T8-2-4	110.36 ± 0.27	462 ± 9	114.3 ± 2.0	0.0241 ± 0.0004	95.4 ± 2.5	2384 ± 42	2276 ± 88	115 ± 2
34-T8-2-5	220.33 ± 0.50	461 ± 9	118.1 ± 2.0	0.0375 ± 0.0034	295.1 ± 27.3	3720 ± 342	3665 ± 344	119 ± 2
34-T8-2-6	520.67 ± 1.26	1101 ± 22	128.3 ± 2.1	0.0249 ± 0.0003	194.3 ± 4.5	2436 ± 28	2382 ± 48	129 ± 2
34-T8-2-7	280.36 ± 0.61	306 ± 6	131.3 ± 2.0	0.0193 ± 0.0002	292 ± 7.0	1873 ± 25	1845 ± 32	132 ± 2
34-T8-2-8	672.58 ± 1.68	2026 ± 41	128.1 ± 2.1	0.0509 ± 0.0003	278.6 ± 5.7	5031 ± 28	4954 ± 61	130 ± 2
20-T8-1-1	316.33 ± 0.62	263 ± 5	144.1 ± 2.1	0.0079 ± 0.0002	157.3 ± 4.9	758 ± 18	737 ± 23	144 ± 2
20-T8-1-2	268.75 ± 0.51	748 ± 69	145.4 ± 2.2	0.1223 ± 0.0209	724.1 ± 140.5	12,285 ± 2218	12,214 ± 2218	151 ± 2
20-T8-1-3	57.69 ± 0.07	140 ± 3	143.7 ± 2.1	0.156 ± 0.0036	1057.8 ± 32.7	15,947 ± 397	15,886 ± 399	150 ± 2
20-T8-4-1	26.74 ± 0.04	327 ± 7	141.8 ± 2.0	0.1157 ± 0.0020	156.3 ± 4.1	11,629 ± 210	11,318 ± 303	146 ± 2
20-T8-4-2	22.53 ± 0.03	244 ± 5	141.5 ± 2.5	0.0926 ± 0.0026	141 ± 4.8	9214 ± 267	8939 ± 330	145 ± 3
20-T8-4-3	25.21 ± 0.03	390 ± 8	139.9 ± 2.2	0.1316 ± 0.0022	140.1 ± 3.7	13,347 ± 239	12,953 ± 367	145 ± 2

Table 1 continued

Sample number	^{238}U (ppb)	^{232}Th (ppt)	δ^{234}U measured[a]	$[^{230}Th/^{238}U]$ activity[b]	$[^{230}Th/^{232}Th]$ 10^{-6}[c]	^{230}Th Age (yr) uncorrected	^{230}Th Age (yr) corrected[d]	$\delta^{234}U_{initial}$ corrected[e]
GBW04412[f]	10,350 ± 17	5004 ± 101	850.3 ± 2.5	1.072 ± 0.0025	36,553.6 ± 741.9	87,118 ± 344	87,111 ± 344	1087 ± 3

Decay constants are 1.55125×10^{-10} for ^{238}U (Jaffey et al. 1971), 2.82206×10^{-6} for ^{234}U and 9.1705×10^{-6} for ^{230}Th (Cheng et al. 2013)

[a] $\delta^{234}U = \left\{\left[\left(\frac{^{234}U}{^{238}U}\right)_{activity} / \left(\frac{^{234}U}{^{238}U}\right)_{equilibrium}\right] - 1\right\} \times 1000$

[b] $\left(\frac{^{230}Th}{^{238}U}\right)_{activity} - 1 = -e^{-\lambda_{230}t} + \frac{\delta^{234}U_{measured}}{1000} \times \frac{\lambda_{230}}{\lambda_{230}-\lambda_{234}}\left[1 - e^{-(\lambda_{230}-\lambda_{234})t}\right]$, where t is the age

[c] The degree of ^{230}Th contamination is indicated by the $[^{230}Th/^{232}Th]$ atomic ratio instead of the activity ratio

[d] Age corrections were calculated using the initial $^{230}Th/^{232}Th$ atomic ratio $4.4 \pm 2.2 \times 10^{-6}$. Those are the values for a material at secular equilibrium, with the bulk earth $^{232}Th/^{238}U$ value of 3.8. The errors are arbitrarily assumed to be 50 %

[e] $\delta^{234}U_{initial}$ corrected was calculated based on ^{230}Th age (t), i.e., $\delta^{234}U_{initial} = \delta^{234}U_{measured} \times e^{-\lambda_{234}t}$, and t is corrected age

[f] GBW04412 is carbonate standard sample for Uranium-series Dating. The men age of GBW04412 for 10 labs is 85,000 (±4000) years (Han 2000)

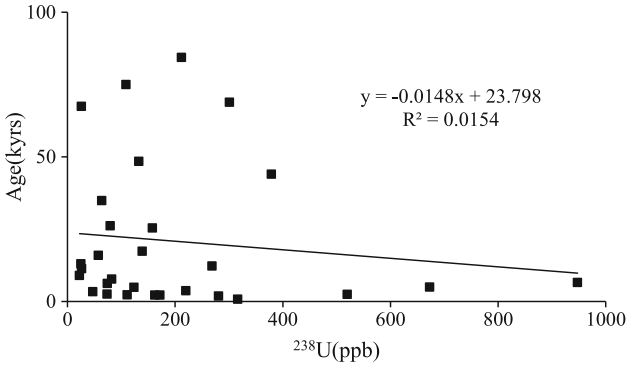

Fig. 3 The relationship between the ^{230}Th age and ^{238}U concentrations for sulfide samples from Duanqiao hydrothermal field. R represents correlation coefficent

(133.61 ± 0.23 ppb), 34-T8-1-11 (79.88 ± 0.12 ppb) is low, but the ages of them are relatively older: 34.8 (±0.3) kyrs, 48.8 (±0.4) kyrs and (26.1 ± 0.2) kyrs, respectively. The U content of sample 34-T8-2-1, 20-T8-4-1, 20-T8-4-2 and 20-T8-4-3 is extremely low, which are 73.65 (±0.24), 26.74 (±0.04), 22.53 (±0.03) and 25.21 (±0.03) ppb respectively, while their ages are 2.5 (±0.1), 11.3 (±0.3), 8.9 (±0.3) and 12.9 (±0.4) kyrs. In some cases, there is a large difference of U content between the subsamples, such as between samples 34-T8-2 and 20-T8-4. All the samples used in this study are the central part of massive and relict chimney sulfide samples to avoid external and the more oxidized parts. All these excludes open system conditions with respect to uranium (Lalou et al. 1998b; Kuznetsov et al. 2015; Mills et al. 1994).

Most of the measured δ^{234}U values range between 104.2 (±2.4) and 187.3 (±2.3) (Table 1). However, samples 34-T8-1-2, 34-T8-1-3, 34-T8-1-7 and 34-T8-1-13 had δ^{234}U values of 239.6 (±2.2), 220.3 (±2.3), 271.5 (±2.1) and 471.7 (±2.6) respectively. The $^{230}Th/^{232}Th$ atomic ratios of relict chimney samples fall within a wide range, from 95.4 (±2.5) × 10^{-6} to 3.186 (±0.065) × 10^{-3}. While the $^{230}Th/^{232}Th$ atomic ratios of massive sulfides span a relatively narrow range, from 140.1 (±3.7) × 10^{-6} to 1.057 (±0.0037) × 10^{-3}. All the ages are corrected with an initial $^{230}Th/^{232}Th$ value of 4.4 (±2.2) × 10^{-6}. The corrected ^{230}Th age of the relict chimney samples vary between 1.845 (±0.032) and 84.3 (±0.5) kyrs while the corrected ^{230}Th age of the massive sulfides range from 0.737 (±0.023) to 15.8 (±0.4) kyrs.

Discussion

U and Th systematics of hydrothermal sulfides from Duanqiao

The ^{232}Th concentrations vary widely across the different section of the relict chimney samples from 244 (±5) to 3363 (±68) ppt. The ^{232}Th concentration of massive sulfides

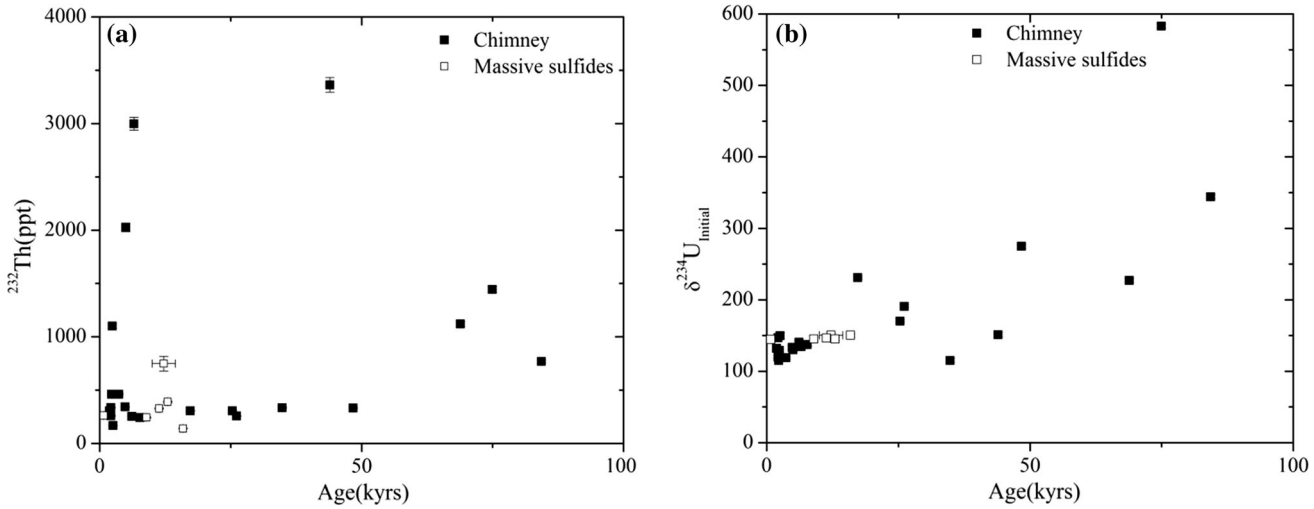

Fig. 4 Temporal variation of U–Th chemistry of sulfides from Duanqiao field. **a** ^{232}Th concentration versus ages. **b** The $\delta^{234}U_{initial}$ of most sulfides of Duanqiao is near the ambient seawater value of 146.5 ± 0.6 (Ludwig et al. 2011)

ranges from 140 (±3) to 748 (±69) ppt. In general, the ^{232}Th of most sulfides from Duanqiao fall in a certain range of 140 to 462 ppt. The thorium concentration sometimes increases with the sulfide age (Fig. 4a), which may be attributed to Th scavenging form ambient Th and Fe–Mn oxides over time (Andersen et al. 2010; Ludwig et al. 2006).

Most $\delta^{234}U_{initial}$ values of sulfides from Duanqiao fall in a range 115 (±3) to 150 (±4), except for a few relict chimney samples with higher $\delta^{234}U_{initial}$ values (Table 1 and Fig. 4b). Chen et al. (1986) found that vent fluid samples collected from black smokers at the 21°N EPR site had $\delta^{234}U$ values of 140–200, while seawater ranged from 149 (±8) to 155 (±17). The vent fluid and seawater from Lost City hydrothermal filed range from 92 (±116) to 183 (±46), 146.1 (±1.5) to 146.9 (±1.4), respectively (Ludwig et al. 2011). The $\delta^{234}U_{initial}$ of modern solitary deep sea corals ranges from 142.9 (±3.2) to 147.2 (±1.1) (Cheng et al. 2000). The $\delta^{234}U_{initial}$ of carbonate chimney samples from Lost City hydrothermal field range from 132.2 (±2.0) to 173 (±17) and the average chimney corrected initial $\delta^{234}U$ is 147.2 (±0.8) (Ludwig et al. 2011). Most $\delta^{234}U_{initial}$ values in our study fall with the range of 115 (±3) to 170 (±2) except for a few relict chimney samples with higher $\delta^{234}U_{initial}$ values which are within the known ranges of seawater and vent fluid (Fig. 4b). This may be caused by the mixing of seawater and fluid during sulfide formation. The uranium in the sulfides from Duanqiao is derived mainly from seawater, if we assume a mixing model using the end-member value of fluid. In this study, we did not have the precise $\delta^{234}U$ data from the seawater, vent fluid, and sediments from seawater of Duanqiao hydrothermal field. We plan to obtain these measurements in future research. It is unclear why the $\delta^{234}U_{initial}$ values of few relict chimney samples like 34-T8-1-7 (344 ± 3) and 34-T8-1-13 (583 ± 3) are high, and deviate considerably from the seawater or well-known sediments from seawater. This also needs to be addressed in further studies.

Age distribution of relict chimney samples

The results of this study provide the first comprehensive analysis of the age distribution of relict chimneys in the SWIR. Most subsamples from the relict chimney section 34-T8-1 range from 4.857 (±0.073) kyrs (sample 34-T8-1-6) to 84.338 (±0.534) kyrs (sample 34-T8-1-7). From inner to outer of chimney section 34-T8-1 (1–4, 6–7, 9–13), the ages show an increasing tendency which may indicate the growth history of the chimney (Fig. 5).

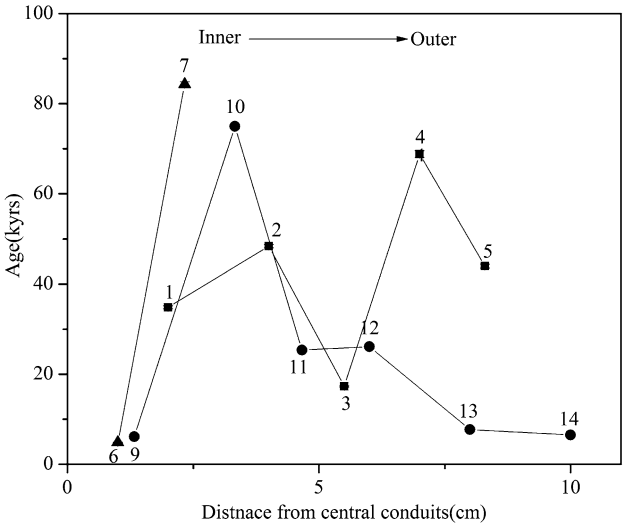

Fig. 5 Age distribution of the relict chimney section 34-T8-1. *Numbers 1–14* represent different parts of the section. *1–5*, *6–7*, *9–14* indicate locations from the inner to outer parts of the conduits of the chimney section. See details in Fig. 2

However, from sample 34-T8-1-4 to 34-T8-1-5 and from sample 34-T8-1-14 to 34-T8-1-15, the age suddenly drops from 80 kyrs to several kyrs. Multi-stage mineralization of the field is very common for many conduits of the relict chimney samples. The mineralogy of Duanqiao indicates that amorphous silica may be precipitated in the later stage of chimney formation. After the chimney collapsed, the reaction of seawater and basalts result the accumulation of new sulfide, which may cause the suddenly change in the composition of the adjacent subsamples.

Compared with chimney section 34-T8-1, the subsamples of chimney section 34-T8-2 are younger and their age distribution is narrow, from 1.845 (±0.032) kyrs to 4.954 (±0.061) kyrs. Sample 34-T8-2-2 near the central conduit of the chimney yielded an age of about 2.150 (±0.046) kyrs (Fig. 2b). Samples 34-T8-2-1 and 34-T8-2-3, which are located away from the central conduit, are older, indicating that the chimney grew from the outer wall to inter wall. However, the $^{230}Th/^{238}U$ ages of samples 34-T8-2-5, 34-T8-2-6, 34-T8-2-7 suggests that it grew from the central to the outside side of the conduit (Fig. 2b).

Estimation of growth rate of the relict chimney

The growth rate of chimney, or mineralization rate, is important to estimate the size of chimney or sulfide ore bodies (Lalou et al. 1998a). The growth rate of chimneys has been estimated by many methods including $^{210}Pb/Pb$, $^{228}Ra/^{226}Ra$ and $^{230}Th/^{234}U$ disequilibrium methods. Kadko et al. (1985) estimated that the growth rate of a chimney from the Juan de Fuca Ridge at 1.2 cm/yr by the $^{210}Pb/Pb$ method. Based on the same method, an axial seamount sulfide chimney from the Juan de Fuca Ridge showed an average growth rate of 3.9 ± 1.9 mm/yr in the earlier stage and 0.51 ± 0.06 mm/yr in the later stage (Kim and McMurty 1991). However the chimney yielded an average growth rate of 6.3 ± 2.1 mm/yr using the $^{228}Ra/^{226}Ra$ method (Kim and McMurty 1991). A barite-rich chimney from Clam Bed Site from Endeavour Segment of the Juan de Fuca Ridge yielded a vertical growth rate of 5.8 cm/yr and a radial growth rate of 2.6 cm/yr by using $^{228}Th/^{228}Ra$ ages (Reyes et al. 1995).

Radioactive nuclides with short half-lives(<1 kyrs) are commonly used to estimate the growth rates of chimneys with rapid growth rates(Reyes et al. 1995). However, the $^{230}Th/^{238}U$ method was used for samples with older ages. Takamasa et al. (2013) firstly demonstrated that a hydrothermal sulfide deposit can continue to grow over a time period of several 1000 years. The growth rate of the barite-containing sulfide crust from South Mariana Trough is less than 0.1 mm/yr. Then Ishibashi et al. (2015) dated core samples from South Mariana Trough and estimated that the growth rate of the massive sulfide were 0.2–1.5 mm/yr. More than 1000 years of continuous hydrothermal activity would be necessary for the formation of a massive sulfide deposit.

The results of this study are the first to estimate the growth rate of relict chimneys and massive sulfide mineralization in the SWIR. According to the results of chimney section of 34-T8-2, it may roughly suggest that sulfide chimney grew continuously from ~4.95 to 2.11 kyrs. The distance from subsamples 34-T8-2-2 and 34-T8-2-7 is about 5 cm (Fig. 2b). If we assume the hydrothermal activity was in steady state in last 4.95 kys, the possible estimated mean growth rate of the sulfide chimney is less than 0.02 mm/yr (Fig. 2a). Stüben et al. (1994) suggested that the age of an inactive silica chimney from the Mariana back-arc spreading center was around 7.5 kyrs, but the growth rate can not be estimated because of the large uncertainties associated with individual ages. Under the similar conditions, with the intermittent hydrothermal activity, it is also difficult to estimate the growth rate of chimney section 34-T8-1. If we assume that the growth was constant in the same time scale, the growth rate would be similar to that obtained for chimney section 34-T8-2.

Episodes of hydrothermal activity

Complete geochronological data for sulfides from Duanqiao hydrothermal field are given in Table 1 and Fig. 2. The oldest sulfide age is 84.338 (±0.534) kyrs, from the northern part of the field. The youngest sulfide with an age of 0.737 (±0.023) kyrs was observed at the middle part of the field. Based on all the results of the two sample locations, four major episodes of hydrothermal activity can be preliminary summarized during the last 80 kyrs (Fig. 6). Hydrothermal activity may started about 84.3 (±0.5) kyrs ago and lasted for about 15 kyrs. After a period of quiescence, around 46.3 kyrs ago, hydrothermalism was

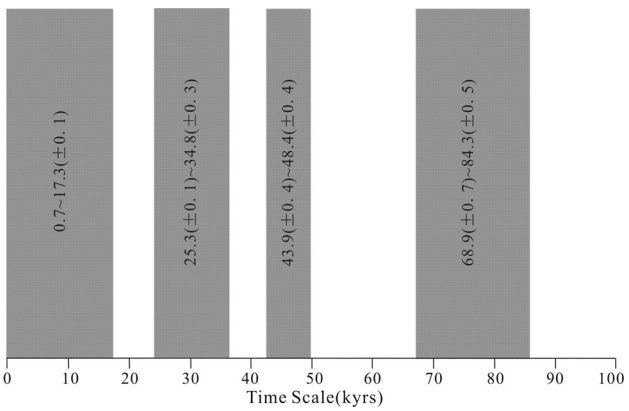

Fig. 6 Four major episodes of hydrothermal activities at Duanqiao hydrothermal field during the last 84.3 kyrs

Table 2 The minimum and maximum ages of sulfide deposits for active and inactive hydrothermal fields of MORs

Location	Deposit	Spreading rate (cm/yr)	Active/ inactive	Numbers of samples dated	Minimum age (kyrs)	Maxiamum age (kyrs)	References
Southwest Indian Ridge	Duanqiao	1.2	Inactive	28	0.737 (±0.023)	84.3 (±0.5)	This study
	Dragon Flag	1.2	Active	6	1.496 (±0.176)	15.9 (±0.2)	Yang et al. submitted for publication
	Mt. Jourdanne	1.4	Inactive	7	12.5 (±0.66)	69.8 (±13.2)	Münch et al. (2001)
Central Indian Ridge	Kairei	4.9	Active	8	0.173	96.3 (±6.1)	Wang et al. (2012)
	Talus Tips	5	Inactive	17	14.7 (±1.56)	140 (±23)	Lalou et al. (1998a)
	Sonne Field	5	Inactive	8	11.8 (±1.5)	20.4 (±1.8)	
Mid-AtlanticRidge	Semyenov	2.6	Inactive	1	–	123.8 (±9.7)	Cherkashov et al. (2010, 2013), Kuznetsov et al. (2011)
	Krasnow	2.6	Inactive	1	–	119.2 (±12.2)	Cherkashev et al. (2008, 2013)
	Zenith-Victoria	2.6	Active?	1	–	59.5 (±8.4)	Cherkashev et al. (2013), Shilov et al. (2012), Kuznetsov et al. (2015)
	Peterburgskoe	2.6	Inactive	8	63 (±5)	176 (±59)	
	Puy des Folles	2.6	Active	1	–	18.2 (±4.4)	Cherkashov et al. (2010)
	Logatchev-1	2.6	Inactive	4	16.5 (±2.1)	58.6 (±4.6)	Kuznetsov et al. (2007)
	Logatchev-2	2.6	Active	1	–	3.9 (±0.4)	
	Rainbow	2.6	Active	4	3.9 (±0.6)	23 (±1.5)	
	16°38′N	2.6	Active	6	33 (±1.7)	61.9 (±2.8)	Shilov et al. (2012)
	Ashadze-1	1.6	Inactive	4	2.1 (±0.3)	7.2 ± 1.8	Kuznetsov et al. (2007)
	Ashadze-2	1.6	Active	5	12.4 (±0.4)	23.4 ± 2.8	
	14°45′N	2.6	Active	16	3.1 (±0.2)	66.5 (±7.0)	Lalou et al. (1996)
	TAG	2.4	Active	60	0.67 (±0.045)	102 (±7)	Lalou et al. (1993, 1995)
	Snakepit	2.4	Active	12	0.875 (±0.1)	4.2 (±0.6)	Lalou et al. (1993)
East Pacific Rise	Endeavour	6	Inactive/Active	44	0.16 (±0.13)	5.85 (±0.21)	Jamieson et al. (2013); Stakes and Moore (1991)
	Northern Cleft	5.8	Inactive/Active	10	0	0.135 (±0.022)	Koski et al. (1994)
	12°50′N	11	Active	5	0.17	20 (±3)	Hannington et al. (1998), Jamieson et al. (2014)

reactivated for a period of 5000 years. Then hydrothermal activity was interrupted for about 10 kyrs. This was followed by the third hydrothermal event, between 25.3 (±0.1) to 34.8 (±0.3) kyrs. The most recent hydrothermal event began at 17.3 (±0.1) kyrs ago. Hydrothermal activity ceased about 0.737 (±0.023) kyrs ago. In the future, we need to collect more samples here to better constrain the episodes of hydrothermal activity of Duanqiao hydrothermal field.

Comparisons with ages of sulfides at other Mid-Oceanic Ridge

Compared with the ages of sulfide ore samples from fast-, intermediate-, and slow- spreading ridges, sulfide ages from the ultraslow spreading center studied in this work are also widely distributed. The ages of 270 sulfides from other mid-oceanic ridge(MOR) sites range from <10 yrs to 200 kyrs. The majority of older sulfides (with ages greater than ~10 kyrs) are from the SWIR(Münch et al. 2001), CIR (Lalou et al. 1998a, b; Wang et al. 2012), MAR (Cherkashev et al. 2013; Cherkashov et al. 2010; Lalou et al. 1993, 1996; Shilov et al. 2012) (Table 2; Fig. 7).

The maximum age of the relict chimneys (84 kyrs) in Duanqiao hydrothermal filed is close to that of the chimneys at Mt. Jourdanne which yielded an age of 70 kyrs (Münch et al. 2001). The ages of the massive sulfides from Duanqiao (0.737 ± 0.023–15.886 ± 0.339 kyrs) are younger than sulfides from most hydrothermal fields such as Rainbow, Sonna and Ashadze-2 (Table 2; Fig. 7). The

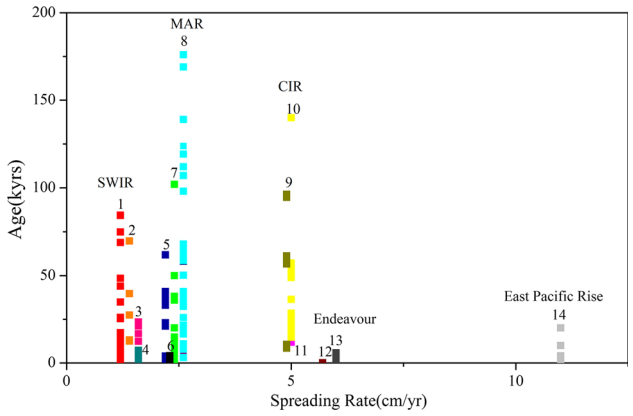

Fig. 7 Plot of the sulfides ages of mid-oceanic ridges and spreading rates. *1*-this study; *2*-Mt. Jourdanne; *3*-Ashadze-2; *4*-Ashadze-1; *5*-Rainbow; *6*-Snakepit; *7*-TAG; *8*-some hydrothermal fields of MAR (including the Semyenov, Kranow, Zenith-Viectoria, Puy Des Folles; Peterburgs; Logatchev-1, Logatchev-2, 16°38′N, 14°45′N); *9*-Kairei; *10*-Talus Tips; *11*-Sonne Field; *12*-Northern Cleft; *13*-Endeavour; *14*-East Pacific Rise(EPR). The sulfides were dated by $^{230}Th/^{238}U$ method, apart from some samples from Endeavour which were dated using the $^{226}Ra/Ba$ method and samples from Northern Cleft Segment, Endeavour and East Pacific Rise that were dated by $^{210}Pb/Pb$ method. The references are shown in Table 2

sulfide ores from Peterburgskoe field of Mid-Atlantic Ridge yielded the oldest age of 176.2 (±59) kyrs (Cherkashev et al. 2013). Most of inactive fields are much older than the active fields. The mean maximum age of inactive fields is 80.52 kyrs while the mean maximum age of active fields is 41.23 kyrs (Table 2).

There is a slight negative trend between the ages of sulfide ore deposits and their spreading rates (Fig. 7). Jamieson et al. (2013) pointed out that this slight anti-correlation may reflect the amount of time a section of ocean curst resides within the hydrothermally active neo-volcanic zone of a spreading center.

There is no age correlation between the hydrothermal events at different sites along the MAR, CIR and SWIR. But there is great similarity between Duanqiao and Mt. Jourdanne from the SWIR. Münch et al. (2001) reconstructed the evolution history of Mt. Jourdanne hydrothermal field. The age dating results indicate activity in two episodes, at 70–40 and 27–13 kyrs. The authors studied the sulfide samples from the nearby Dragon Flag filed at the same time and the results show that the ages of most sulfides from Dragon Flag field range from 1.496 (±0.176) to 5.416 (±0.116) kyrs with the oldest age estimated at 15.997 (±0.155) kyrs (Yang et al. submitted for publication). All these results suggest that hydrothermal activity of Dragon Flag field is much more recent than that of Duanqiao or Mt. Jourdanne fields.

Mt. Jourdanne is situated on an axial volcanic ridge which has both volcanic and tectonic activity. This is necessary to develop the heat source and pathways for the fluid convection, which enables the hydrothermal circulation (Münch et al. 2001). Hydrothermal activity in Dragon Flag Field is located next to the detachment fault termination. The detachment fault system provides a pathway for hydrothermal convection (Sauter et al. 2009; Tao et al. 2012; Zhao et al. 2013). Such style of heat source can contribute to continuous hydrothermal activity for over 1000 years. Duanqiao field is located near the central volcano and there is a hot mantle and/or fertile melt beneath Duanqiao field (Tao et al. 2012; Niu et al. 2015). The crust thickness is 9.5 km, suggesting the existence of AMC (Axial Magma Chamber) which provides magma source to the field (Li et al. 2015; Mendel et al. 2003). The periodic hydrothermal activity at Duanqiao may be related to the heat source provided by the local interaction of magmatism and tectonism.

Cherkashev et al. (2013) compared data on the size and age of ore fields from MAR and suggested that the time parameter is crucial for the scale of ore formation. Jamieson et al. (2014) plotted the minimum ages of the deposit and the mass accumulation rates and indicated that the accumulation rates of inactive hydrothermal fields are lower than those of most active sulfides. According to the

minimum and maximal accumulation rate of an inactive hydrothermal field (10 t/yr for MESO and 65 t/yr for Semyenov), the preliminarily estimated reserves of sulfide ores of Duanqiao are approximately 0.5–2.9 million tons.

Conclusions

In this study, $^{230}Th/^{238}U$ dating method was applied to sulfides from Duanqiao hydrothermal filed of the SWIR. Twenty-eight sulfides subsamples including relict chimneys subsamples and massive subsamples were analyzed. A complementary geochronological study of hydrothermal sulfides from this hydrothermal field was done.

1. The ^{238}U concentrations of sulfides range from 22.53 (±0.03) to 948.72 (±1) ppb and the ^{232}Th concentrations vary from 140 (±3) to 3363 (±68) ppt. There is no correlation between the ^{230}Th age and the ^{238}U concentrations which excludes an scenario of open system conditions with respect to uranium.
2. The ages of most subsamples from relict chimney section 34-T8-1 range from 4.857 (±0.073) to 84.338 (±0.534) kyrs. From inner to outer of chimney section 34-T8-1, the ages show an increasing tendency, which may indicate the growth history. And the age distribution of section 34-T8-2 is narrow, from 1.845 (±0.032) to 4.954 (±0.061) kyrs.
3. The results of this study are the first to estimate the growth rate of chimneys in the SWIR. Based on the results of chimney section of 34-T8-2, the possible mean growth rate for sulfide chimney is less than 0.02 mm/yr. For the intermittent hydrothermal activity, it is difficult to estimate the growth rate of chimney section of 34-T8-1.
4. Four major episodes of hydrothermal activity can be preliminary summarized: 68.9–84.3, 43.9–48.4, 25.3–34.8, and 0.7–17.3 kyrs. The periodic character of hydrothermal activity may be related to the heat source provided by the interaction of magmatism and tectonism.
5. There is great similarity between Duanqiao and Mt. Jourdanne from Southwest Indian Ridge. The maximum age of relict chimneys (84 kyrs) in Duanqiao hydrothermal filed is close to the chimneys from Mt. Jourdanne which yielded an age of 70 kyrs. The hydrothermal activity in Dragon Flag field is much more recent than that of Duanqiao or Mt. Jourdanne field. The ages of massive sulfides from Duanqiao are younger than sulfides from most hydrothermal fields such as Rainbow, Sonne and Ashadze-2. The preliminarily estimated reserves of sulfide ores of Duanqiao are approximately 0.5–2.9 million tons.

Acknowledgments We would like to thank the captains, crew and the science parties who participated the DY115-20 and DY125-34 cruises on Dayang Yihao. This study was financially supported by National Basic Research Program of China (973 Program) under contract No. 2012CB417305, China Ocean Mineral Resources R & D Association "Twelfth Five-Year" Major Program under contract No. DY125-11-R-01 and DY125-11-R-05, Zhejiang Provincial Natural Science Foundation of China under Grant No. Q16D060018, the National Program on Global Change and Air-Sea Interaction, SOA (No. GASI-GEOGE-01), and MOST of China (No. 2016YFC 0600402). We would also like to thank Professor Edward T. Baker and Chuanwan Dong for constructive comments on our paper.

References

Andersen MB, Stirling CH, Potter EK, Halliday AN, Blake SG, McCulloch MT, Ayling BF, O'Leary M (2008) High-precision U-series measurements of more than 500,000 year old fossil corals. Earth Planet Sci Lett 265:229–245. doi:10.1016/j.epsl.2007.10.010

Andersen MB, Stirling CH, Zimmermann B, Halliday A (2010) Precise determination of the open ocean $^{234}U/^{238}U$ composition[J]. Geochem Geophys Geosyst 11(12): doi:10.1029/2010GC003318

Baker ET, German CR (2004) On the global distribution of hydrothermal vent fields. In: German CR, Lin J, Parson LM (eds) Mid-ocean ridges: hydrothermal interactions between the lithosphere and oceans. AGU, Washington, pp 245–266. doi:10.1029/148GM10

Cannat M, Rommevaux-Jestin C, Fujimoto H (2003) Melt supply variations to a magma-poor ultra-slow spreading ridge (Southwest Indian Ridge 61° to 69°E). Geochem Geophys Geosyst 4(8):9104–9125. doi:10.1029/2002GC000480

Chen JH, Wasserburg GJ, Von Damm KL, Edmond JM (1986) The U–Th–Pb systematics in hot springs on the East Pacific Rise at 21°N and Guaymas Basin. Geochim Cosmochim Acta 50:2467–2479. doi:10.1016/0016-7037(86)90030-X

Cheng H, Adkins J, Edwards RL, Boyle EA (2000) U–Th dating of deep-sea corals. Geochim Cosmochim Acta 64(14):2401–2416

Cheng H, Edwards RL, Shen CC, Woodhead J, Hellstrom J, Wang YJ, Kong XG, Spötl C, Wang XF, Alexander EC Jr (2013) Improvements in ^{230}Th dating, ^{230}Th and ^{234}U half-life values, and U–Th isotopic measurements by multi-collector inductively coupled plasma mass spectrometry. Earth Planet Sci Lett 371–372:82–91. doi:10.1016/j.epsl.2013.04.006

Cherkashev G, Bel'tenev V, Ivanov V, Lazareva L, Samovarov M, Shilo V, Stepanova T, Glasby GP, Kuznetsov V (2008) Two new hydrothermal fields at the Mid-Atlantic Ridge. Mar Georesour Geotechnol 26(4):308–316. doi:10.1080/10641190802400708

Cherkashev GA, Ivanov VN, Bel'tenev VI, Lazareva LI, Rozhdestvenskaya II, Samovarov ML, Poroshina IM, Sergeev MB, Stepanova TV, Dobretsova IG, Kuznetsov VY (2013) Massive Sulfide ores of the northern equatorial Mid-Atlantic Ridge. Oceanology. 53(5):607–619. doi:10.1134/S0001437013050032

Cherkashov G, Poroshina I, Steopanova T, Ivanov V, Bel'tenev V, Lazareva L, Rozhdestvenskaya I, Samovarov M, Shilov V, Glasby GP, Fouquet Y, Kuznetsov V (2010) Seafloor massive sulfides from the northern equatorial Mid-Atlantic Ridge: new discoveries and perspectives. Mar Georesour Geotechnol 28:222–239. doi:10.1080/1064119X.2010.483308

Dick HJB, Lin J, Schouten H (2003) An ultraslow-spreading class of ocean ridge. Nature 426:405–412. doi:10.1038/nature02128

Edwards RL, Chen JH, Ku T-L, Wasserburg GJ (1987) Precise timing of the last interglacial period from mass spectrometric analysis of ^{230}Th in corals. Science 236:1537–1553. doi:10.1126/science.236.4808.1547

Georgen JE, Lin J, Dick HJB (2001) Evidence from gravity anomalies for interactions of the Marion and Bouvet hotspots with the Southwest Indian Ridge: Effects of transform offsets. Earth Planet Sci Lett 187:283–300. doi:10.1016/S0012-821X(01)00293-X

Georgen JE, Kurz MD, Dick HJB, Lin J (2003) Low ^{3}He/^{4}He ratios in basalt glasses from the western Southwest Indian Ridge (10°–24°E). Earth Planet Sci Lett 206:509–528. doi:10.1016/S0012-821X(02)01106-8

Han YZ (2000) Catalogue of the standard materials of the People's Republic of China, vol 55. China Metrology Publishing House, New York

Hannington M, Galley A, Herzig P, Petersen S (1998) Comparison of the TAG mound and stockwork complex with Cyprus-type massive sulfide deposits. In: Herzig PM, Humphris SE, Miller DJ, Zierenberg RA (eds) Proceedings of ODP, science results, vol 158, pp 389–415

Ishibashi J, Shimada K, Sato F, Uchida A, Toyoda S, Takamasa A, Nakai S, Hyodo H, Sato K, Kumagai H, Ikehata K (2015) Dating of hydrothermal mineralization in active hydrothermal fields in the southern mariana trough. In: Subseafloor biosphere linked to hydrothermal systems: taiga concept, pp 289–300. doi:10.1007/978-4-431-54865-2-23

Jaffey AH, Flymn KF, Glendenin LE, Bentley WC, Essling AM (1971) Precision measurement of high-lives and specific activities of ^{235}U and ^{238}U. Phys Rev C4:1889–1906

Jamieson JW, Hannington LE, Clague DA, Kelley DS, Delaney JR, Holden JR, Tivey MK, Kimpe LE (2013) Sulfide geochronology along the Endeavour Segment of the Juan de Fuca Ridge. Geochem Geophys Geosyst 14:2084–2099. doi:10.1002/ggge.20133

Jamieson JW, Clague DA, Hannington MD (2014) Hydrothermal sulfide accumulation along the Endeavour Segment, Juan de Fuca Ridge. Earth Planet Sci Lett 395:136–148. doi:10.1016/j.epsl.2014.03.035

Kadko D, Koski R, Tatsumoto M, Bouse R (1985) An estimate of hydrothermal fluid residence times and vent chimney growth rates based on ^{210}Pb/Pb ratios and mineralogic studies of sulfides dredged from the Juan de Fuca Ridge. Earth Planet Sci Lett 76:35–44. doi:10.1016/0012-821X(85)90146-3

Kasuya M, Kato M, Ikeya M (1991) ESR signals of natural barite ($BaSO_4$) crystals: possible application to geochronology. In: Essay in geology, Prof. Nakagawa Commemorative, vol 95–98

Kim KH, McMurty GM (1991) Radial growth rates and ^{210}Pb ages of hydrothermal massive sulfides from the Juan de Fuca Ridge. Earth Planet Sci Lett 104:299–314. doi:10.1016/0012-821X(91)90211-Y

Koski RA, Jonasson IR, Kadko DC, Smith VK, Wong FL (1994) Compositions, growth mechanisms, and temporal relations of hydrothermal sulfide-sulfate-silica chimneys at the northern Cleft segment, Juan de Fuca Ridge. J Geophys Res Solid Earth 99(B3):4813–4832

Kuznetsov V, Cherkashev G, Lein A, Shilov V, Maksimov F, Arslanov Kh, Stepanova T, Baranova N, Chernov S, Tarasenko D (2006) ^{230}Th/U dating of massive sulfides from the Logatchev and Rainbow hydrothermal fields (Mid-Atlantic Ridge). Geochronometria 25:51–56

Kuznetsov V, Cherkashev G, Bel Tenev V, Lein A, Maximov F, Shilov V, Stepanova T (2007) The ^{230}Th/U dating of sulfide ores in the ocean: methodical possibilities, measurement results, and perspectives of application. Dokl Earth Sci 417:1202–1205. doi:10.1134/S1028334X07080156

Kuznetsov V, Maksimov F, Zheleznov A, Cherkashov G, BelTenev V, Lazareva L (2011) ^{230}Th/U chronology of ore formation within the semyenov hydrothermal district (13°31′N) at the Mid-Atlantic ridge. Geochronometria 38:72–76. doi:10.2478/s13386-011-0001-1

Kuznetsov VY, Tabuns EV, Bel'tenev VE, Cherkashev GA, Maksimov FE, Kuksa KA, Baranova NG, Levchenko SB (2013) ^{230}Th/U Chronology of seafloor massive sulfides formation within the Zenith-Victoria ore field. Bull St Petersb State Univ 4(7):119–130 **(in Russian, with abstract in English)**

Kuznetsov V, Tabuns E, Kuksa K et al (2015) The oldest seafloor ore massive sulfide deposits at the Mid-Atlantic ridge: ^{230}Th/U chronology and composition. Geochronometria 42:100–106. doi:10.1515/geochr-2015-0009

Lalou C, Brichet E (1982) Age and implication of East Pacific Rise sulphide deposits at 21°N. Nature (London) 300(5888):169–171. doi:10.1038/300169a0

Lalou C, Brichet E (1987) On the isotopic chronology of submarine hydrothermal deposits. Chem Geol 65:197–207. doi:10.1016/0168-9622(87)90003-0

Lalou C, Brichet E, Hekinian R (1985) Age dating of sulfide deposits from axial and off-axial structures on the East Pacific Rise near 12°50′N. Earth Planet Sci Lett 75:59–71. doi:10.1016/0012-821X(85)90050-0

Lalou C, Thompson G, Rona PA, Brichet E (1986) Chronology of selected hydrothermal Mn oxide deposits from the Transatlantic Geotraverse "TAG" area. Geochim Cosmochim Acta 50:1737–1743. doi:10.1016/0016-7037(86)90135-3

Lalou C, Reyss J, Brichet E, Arnold M, Thompson G, Fouquet Y, Rona PA (1993) New age data for Mid-Atlantic Ridge hydrothermal sites: TAG and Snakepit chronology revisited. J Geophys Res 98:9705–9713. doi:10.1029/92JB01898

Lalou C, Reyss JL, Brichet E, Rona PA, Thompson G (1995) Hydrothermal activity on a 10^5-year scale at a slow-spreading ridge, TAG hydrothermal field, Mid-Atlantic Ridge 26° N[J]. J Geophys Res Solid Earth 100(B9):17855–17862

Lalou C, Reyss J, Brichet E, Krasnov S, Stepanova T, Cherkashev G, Markov V (1996) Initial chronology of a recently discovered hydrothermal field at 14°45′N, Mid-Atlantic Ridge. Earth Planet Sci Lett 144:483–490. doi:10.1016/S0012-821X(96)00190-2

Lalou C, Münch U, Halbach P, Reyss J (1998a) Radiochronological investigation of hydrothermal deposits from the MESO zone, Central Indian Ridge. Mar Geol 149:243–254. doi:10.1016/S0025-3227(98)00042-5

Lalou C, Reyss JL, Brichet E (1998b) Age of sub-bottom sulfides samples at the TAG active mound. In: Proceedings of the ocean drilling program, scientific results, 158

Li JW, Peng XT, Zhou HY, Li JT, Sun ZL (2013) Molecular evidence for microorganisms participating in Fe, Mn, and S biogeochemical cycling in two low-temperature hydrothermal fields at the Southwest Indian Ridge. J Geophys Res Biogeosci 118:665–679. doi:10.1002/jgrg.20057

Li JB, Jian HC, Chen YSJ, Singh SC, Ruan AG, Qiu XL, Zhao MH, Wang XG, Niu XW, Ni JY, Zhang JZ (2015) Seismic observation of an extremely magmatic accretion at the ultraslow spreading Southwest Indian Ridge. Geophys Res Lett 42:2563–2663. doi:10.1002/2014GL062521

Ludwig KA, Kelley DS, Butterfield DA, Nelson BK, Früh-Green GL (2006) Formation and evolution of carbonate chimneys at the Lost City Hydrothermal Field. Geochim Cosmochim Acta 70:3625–3645. doi:10.1016/j.gca.2006.04.016

Ludwig KA, Shen C, Kelley DS, Cheng H, Edwards RL (2011) U–Th systematics and 230Th ages of carbonate chimneys at the Lost City Hydrothermal Field. Geochim Cosmochim Acta 75:1869–1888. doi:10.1016/j.gca.2011.01.008

Mendel V, Sauter D, Rommevaux-Jestin C, Patriat P, Lefebvre F, Parson LM (2003) Magmato-tectonic cyclicity at the ultra-slow spreading Southwest Indian Ridge: evidence from variations of axial volcanic ridge morphology and abyssal hills pattern[J]. Geochem Geophys Geosyst 4:9102. doi:10.1029/2002GC000417

Meyzen CM, Ludden JN, Humler E, Luais B, Toplis MJ, Mével C, Storey M (2005) New insights into the origin and distribution of the DUPAL isotope anomaly in the Indian Ocean mantle from MORB of the Southwest Indian Ridge. Geochem. Geophys. Geosyst. 6:Q11K11. doi:10.1029/2005GC000979

Mills RA, Thomson JM, Elderfield H, Hinton RW, Hyslop E (1994) Uranium enrichment in metalliferous sediments from the Mid-Atlantic Ridge. Earth Planet Sci Lett 124:25–47. doi:10.1016/0012-821X(94)00083-2

Münch U, Blum N, Halbach P (1999) Mineralogical and geochemical features of sulfide chimneys from the MESO zone, Central Indian Ridge. Chem Geol 155:29–44. doi:10.1016/S0009-2541(98)00139-9

Münch U, Lalou C, Halbach P, Fujimoto H (2001) Relict hydrothermal events along the super-slow Southwest Indian spreading ridge near 63°56′E-mineralogy, chemistry and chronology of sulfide samples. Chem Geol 177:341–349. doi:10.1016/S0009-2541(00)00418-6

Niu X, Ruan A, Li J, Minshull TA, Sauter D, Wu Z, Qiu X, Zhao M, Chen YJ, Singh S (2015) Along axis variation in crustal thickness at the ultraslow spreading Southwest Indian Ridge (50°E) from a wide-angle seismic experiment. Geochem Geophys Geosyst 16:468–485. doi:10.1002/2014GC005645

Okumura T, Toyoda S, Sato F, Uchida A, Ishibashi J, Nakai S (2010) ESR dating of marine barites in chimneys deposited from hydrothermal vents. Geochronometria 37:57–61. doi:10.2478/v10003-010-0019-z

Reyes AO, Moore WS, Stakes DS (1995) Th-228/Ra-228 ages of a barite-rich chimney from the Endeavour Segment of the Juan-de-Fuca Ridge. Earth Planet Sci Lett 131(1–2):99–113. doi:10.1016/0012-821X(95)00009-2

Sauter D, Cannat M (2010) The ultraslow spreading southwest Indian ridge: diversity of hydrothermal systems on slow spreading ocean ridges, pp 153–173. doi:10.1029/2008GM000843

Sauter D, Carton H, Mendel V, Munschy M, Rommevaux-Jestin C, Schott J, Whitechurch H (2004) Ridge segmentation and the magnetic structure of the Southwest Indian Ridge (at 50°30′E, 55°30′E and 66°20′E): Implications formagmatic processes at ultraslow-spreading centers. Geochem Geophys Geosyst 5:8. doi:10.1029/2003GC000581

Sauter D, Cannat M, Meyzen C, Bezos A, Patriat P, Humler E, Debayle E (2009) Propagation of a melting anomaly along the ultra-slow Southwest Indian Ridge between 46°E and 52°20′E: interaction with the Crozet hot-spot ? Geophys J Int. doi:10.1111/j.1365-246X.2009.04308.x

Shen CC, Li KS, Sieh K, Natawidjaja D, Cheng H, Wang X, Edwards RL, Lam DD, Hsieh YT, Fan TY, Melzner A, Taylor FW, Quinn TM, Chiang H-W, Kilbourne KH (2008) Variation of initial 230Th/232Th and limits of high precision U–Th dating of shallow-water corals. Geochim Cosmochim Acta 72:4201–4223. doi:10.1016/j.gca.2008.06.011

Shen CC, Lin K, Duan WH, Jiang XY, Partin JW, Edwards RL, Cheng H, Tan M (2013) Testing the annual nature of speleothem banding. Sci Rep 3:2633. doi:10.1038/srep02633

Shilov V, Bel'tenev V, Ivanov V, Cherkashev G, Rozhdestvenskaya I, Gablina I, Dobretsova I, Narkevskiy E, Gustaitis A, Kuznetsov V (2012) New hydrothermal ore fields in the Mid-Atlantic Ridge: Zenith-Victoria (20°08′ N) and Petersburg (19°52′ N). Dokl Earth Sci 442(1):63–69. doi:10.1134/S1028334x12010308

Stakes D, Moore WS (1991) Evolution of hydrothermal activity on the Juan-de-Fuca Ridge: observations, mineralages, and Ra isotope ratios. J Geophys Res 96:21739–21752. doi:10.1029/91JB02038

Stüben D, Taibi NE, McMurty GM, Scholten J, Stoffers P, Zhang D (1994) Growth history of a hydrothermal silica chimney from the Mariana backarc spreading center (southwest Pacific, 18°13′N). Chem Geol 113:273–296. doi:10.1016/0009-2541(94)90071-X

Sun ZL, Li J, Huang W, Dong HL, Little CTS, Li JW (2015) Generation of hydrothermal Fe–Si oxyhydroxide deposit on the Southwest Indian Ridge and its implication for the origin of ancient banded iron formations. J Geophys Res Biogeosci 120:187–203. doi:10.1002/2014JG002764

Takamasa A, Nakai SI, Sato F, Toyoda S, Banerjee D, Ishibashi J (2013) U–Th radioactive disequilibrium and ESR dating of a barite-containing sulfide crust from South Mariana Trough. Quat Geochronol 15:38–46. doi:10.1016/j.quageo.2012.12.002

Tao CH, Lin J, Guo SQ, Chen YSJ, Wu GH, Han XQ, German CR, Yoerger DR, Zhou N, Li HM, Su X, Zhu J (2012) First active hydrothermal vents on an ultraslow spreading center: Southwest Indian Ridge. Geology 40(1):47–50. doi:10.1130/G32389.1

Tao CH, Li HM, Jin XB, Zhou JP, Wu T, He YH, Deng XM, Gu CH, Zhang GY, Liu WY (2014) Seafloor hydrothermal activity and polymetallic sulfide exploration on the southwest Indian ridge. Chin Sci Bull 59(19):2266–2276. doi:10.1007/s11434-014-0182-0

Wang YJ, Han XQ, Jin XL, Qiu ZY, Ma ZB, Yang HL (2012) Hydrothermal activity events at Kairei field, Central Indian Ridge 25°S. Resour Geol 62(2):208–214. doi:10.1111/j.1751-3928.2012.00189.x

Wang LS, Ma ZB, Cheng H, Duan WH, Xiao JL (2016) Determination of ^{230}Th age of Uranium-series standard samples by multiple collector inductively coupled plasma mass spectromerty. J Chin Mass Spectrom Soc 37(3):262–272. doi:10.7538/zpxb.youxian.2016

You CF, Bickle MJ (1998) Evolution of an active sea-floor massive sulphide deposit. Nature 394:668–671. doi:10.1038/29279

Zhao MH, Qiu XL, Li JB, Sauter D, Ruan AG, Chen J, Cannat M, Singh S, Zhang JZ, Wu ZL, Niu XW (2013) Three-dimensional seismic structure of the Dragon Flag oceanic core complex at the ultraslow spreading Southwest Indian Ridge (49°39′E). Geochem Geophys Geosyst 14:4544–4563. doi:10.1002/ggge.20264